

# Evidence for Planet-induced Chromospheric Activity on HD 179949

E. Shkolnik<sup>1</sup> and G.A.H. Walker<sup>1</sup>

*Department of Physics & Astronomy, University of British Columbia, 6224 Agricultural  
Rd., Vancouver BC, Canada V6T 1Z1*

shkolnik@astro.ubc.ca

walker@astro.ubc.ca

and

D.A. Bohlender<sup>1</sup>

*Herzberg Institute for Astrophysics, National Research Council of Canada  
Victoria BC, Canada V9E 2E7*

david.bohlender@nrc-cnrc.gc.ca

## ABSTRACT

We have detected the synchronous enhancement of Ca II H & K emission with the short-period planetary orbit in HD 179949. High-resolution spectra taken on three observing runs extending more than a year show the enhancement coincides with  $\phi \sim 0$  (the sub-planetary point) of the 3.093-day orbit with the effect persisting for more than 100 orbits. The synchronous enhancement is consistent with planet-induced chromospheric heating by magnetic rather than tidal interaction. Something which can only be confirmed by further observations. Independent observations are needed to determine whether the stellar rotation is synchronous with the planet's orbit. Of the five 51 Peg-type systems monitored, HD 179949 shows the greatest chromospheric H & K activity. Three others show significant nightly variations but the lack of any phase coherence prevents us saying whether the activity is induced by the planet. Our two standards,  $\tau$  Ceti and the Sun, show no such nightly variations.

*Subject headings:* stars: activity, chromospheres, planetary systems

---

<sup>1</sup>Visiting Astronomer, Canada-France-Hawaii Telescope, operated by the National Research Council of Canada, the Centre National de la Recherche Scientifique of France, and the University of Hawaii.

## 1. Introduction

Current planet detection methods provide basic information: a minimum mass if the orbital inclination is not known and an albedo-dependent estimate of surface temperature. In the case of the transiting system, HD 209458, the planet’s density is also determined with a possible atmospheric sodium detection (Charbonneau 2002) and excess Lyman  $\alpha$  absorption during transit (Vidal-Madjar et al. 2003). There still remains a lack of constraints on extrasolar planetary structure leaving astronomers to explore new observational probes.

Cuntz, Saar & Musielak (2000) suggested that there may be an observable interaction between a parent star and a close-in giant planet, specifically an external heating of the star’s outer atmosphere. The effect could be tidal, magnetic, or a combination of the two. In the case of tidal heating, the acoustic wave energy thought to contribute to the heating of the upper atmosphere has a dependence on the local turbulent velocity ( $v_t$ ) as  $v_t^8$  (Muzielak et al. 1994). The steepening of the density gradient in the two tidal bulges would increase the turbulent velocity producing excess shocks, waves, and flows in the upper atmosphere of the star. Magnetic wave energy has a  $v_t^6$  dependence (Ulmschneider & Muzielak 1998) such that an increase in  $v_t$  would enhance local dynamo generation and hence the local magnetic energy will also increase. Thus, even small increases in  $v_t$  would cause a dramatic intensification in nonradiative heating. If planet-induced heating is confined to a narrow range in stellar longitude, the heated regions would track the planet. This implies that the period of any observed activity would be correlated with the planet’s orbit such that tidally induced activity has a period of  $\sim P_{orb}/2$  and magnetic activity, a period of  $\sim P_{orb}$ . It is also possible that the increased dynamo action would be confined to the turbulent layer below the convection zone (the tachocline). In this case, any dynamo action would be spread out over a wide range of longitudes and the excess heating would not show strong periodic variation (Saar & Cuntz 2001).

Since the tidal and magnetic interaction depend on the distance from the planet to the star as  $1/d^3$  and  $1/d^2$ , respectively, it is best to look at the tightest systems. Of the  $\sim 100$  known extrasolar planets, 16% have semi-major axes of less than 0.1 AU and masses comparable to Jupiter’s (Schneider 2003). It is expected that these planets have magnetic fields similar to Jupiter’s (4.3 G). However if tidally locked, the planets’ fields might be substantially smaller. It is also reasonable to assume that the magnetic interaction would be greatest in the outermost layers of the star, namely the chromosphere, transition region and the corona due to their proximity to the planets and their nonradiative heat sources. Our program stars have orbital periods between 3.1 and 4.6 days, eccentricities  $\sim 0$  and semi-major axes  $< 0.06$  AU. These systems offer the best chance of observing upper atmospheric heating. The five systems we chose were  $\tau$  Boo, HD 179949, HD 209458, 51 Peg and  $v$  And

and their planetary system parameters are listed in Table 1.

## 2. Chromospheres and Ca II H & K Emission

Temperatures in the chromosphere can reach 20,000 K over many scale heights implying that the temperature gradients are not very high. This is due to the large opacity of resonance lines such as H I, Ca II, Mg II and the Lyman continuum which then in the low-density gas radiate and cool the chromosphere. Most chromospheric indicators are UV emission lines not easily accessible from ground-based telescopes. However, the optical resonance lines of Ca II H & K at 3933 Å and 3968 Å exhibit chromospheric emission in late-type stars (later than F0) and are sensitive probes of temperature and electron density. An example of HD 179949 Ca II H & K reversals are shown in Figure 1. The double-peaked emission is formed in the chromosphere at  $T \sim 8000$  K where the source function is essentially monochromatic. The central emission is produced at a temperature of  $\sim 20,000$  K (Montes et al. 1994) which appears as a self-reversal due to the large optical depth of the line. The asymmetry of the emission in late-type dwarfs is thought to be a consequence of upflows in the chromosphere’s plage-like regions. (See Linsky 1980 for a comprehensive observational and theoretical review.)

The broad, deep photospheric absorption and the low level background continuum allow the reversal to be seen at higher contrast. Because of these and the accessibility of the lines from the ground, the Ca II H & K reversals are an optimal choice with which to monitor chromospheric heating for the sun-like stars known to host short-period giant planets. Saar and Cuntz (2001) looked at the Ca II IR line at 8662 Å, an interlocking line with the Ca II H & K resonance lines, with spectra of resolution  $R = 50,000$  and S/N typically of 200. They looked at five stars with close-in giant planets (including  $\tau$  Boo,  $\nu$  And, and 51 Peg) by simulating the IR equivalent to the Mt. Wilson  $S_{HK}$  index and found nothing at the 3 to 5% level.

## 3. Observations

High-resolution ( $R = 110,000$ ) and high signal-to-noise ( $S/N \approx 500$  per pixel in the continuum and 150 in the H & K cores) spectra were obtained on 3 observing runs at the Canada-France-Hawaii Telescope (CFHT) with the fiber-fed coudé spectrograph, *Gecko*. The single spectrum spanned 60 Å and was centered on 3947 Å. A representative spectrum of HD 179949 is shown in Figure 1. Five nights were allocated in each of three semesters:

August 2001, July 2002 and August 2002. Poor weather and technical issues limited usable data to  $\sim 10$  nights. Spectra with comparable S/N were taken of two stars known not to have close-in giant planets,  $\tau$  Ceti and the Sun (sky spectra were taken at dusk).

The data reduction consisted of the subtraction of the appropriate darks from the stellar, arc and flat-field exposures rather than using the conventional biases to remove the baseline from each observation. The flats were combined and normalized to a mean value of 1 along each row of the dispersion axis. All the stellar exposures for each night were averaged in order to define a single aperture to use for the spectral extraction. This included a subtraction of the residual background level between orders. The aperture was used to extract 1-dimensional spectra from the stellar, comparison and flat-field exposures. A mean, normalized 1-dimensional flat was divided into the extracted spectra to obtain the most consistent flat-fielded spectra possible. The wavelength calibration was done with Thorium-Argon arcs. Heliocentric and differential radial velocity corrections were applied.

In 2001 Th-Ar arcs were taken with every target while in the 2002 observing runs, each stellar exposure was bracketed with an arc. This allowed differential radial velocities ( $\Delta RV$ ) to be measured to better than 20 m/s. Detailed discussion on the  $RV$  can be found in Walker et al. (2003). Current orbital ephemerides and hence accurate phases ( $\pm 0.03$ ) were determined for each observation by fitting a least-squares sine function with the known radial velocity amplitude and orbital period. A pure sinusoid was sufficient since all five systems have eccentricity  $e \leq 0.05$  (Schneider 2003). Table 2 contains the July 2002 times of sub-planetary position along with the revised periods.

For each star, portions of the spectra, each 7 Å wide, were extracted centered on Ca II H, K and the strong Al I line at 3944 Å. As a means of normalizing each sub-spectrum, the continuum was set to 1 at the ends and fit with a straight line. The spectra were grouped by date and a nightly mean was computed for each of the three lines. An overall average was then taken over all the nights from which we measured nightly residuals. Each residual spectrum also had a broad, low-order curvature removed.

## 4. Results

The program stars were originally chosen for Doppler planet searches because of their weak chromospheric activity as indicated by the modest Ca II H & K emission flux measured by the Mt. Wilson  $S_{HK}$  index. However there are marked differences in the reversal structure of each of these targets caused by their different rotational rates (which produce a range of emission strengths and Doppler broadening) as well as by other intrinsic mechanisms,

Table 1. The Program Stars

Star	Spectral Type	$v \sin i^a$ km s <sup>-1</sup>	$M_p \sin i^b$ $M_J$	$P_{orb}^b$ days	Semi-major axis <sup>b</sup> AU	Ca II K Flux <sup>c</sup> Å
$\tau$ Boo	F7 VI	$14.8 \pm 0.3$	3.87	3.3128	0.046	0.326
HD 179949	F8 V	$6.3 \pm 0.9$	0.84	3.093	0.045	0.358
HD 209458	G0 V	$4.2 \pm 0.5$	0.69 <sup>d</sup>	3.524738	0.045	0.192
51 Peg	G2 IV	$2.4 \pm 0.3$	0.47	4.2293	0.05	0.177
$\nu$ And	F7 V	$9.0 \pm 0.4$	0.71 <sup>e</sup>	4.617	0.059	0.252
$\tau$ Cet	G8 V	< 2	–	–	–	0.201
Sun	G2 V	$1.73 \pm 0.3$	–	–	–	0.300

<sup>a</sup> $v \sin i$  references:  $\tau$  Boo (Gray 1982), HD 179949 (Groot et al. 1996), HD 209458 (Mazeh et al. 2000), 51 Peg and Sun (François et al. 1996),  $\nu$  And (Gray 1986),  $\tau$  Ceti (Fekel 1997)

<sup>b</sup>published orbital solutions:  $\tau$  Boo &  $\nu$  And (Butler et al. 1997), HD 179949 (Tinney et al. 2000), 51 Peg (Marcy et al. 1996), HD 209458 (Charbonneau et al. 1999)

<sup>c</sup>total integrated flux of mean normalized K core

<sup>d</sup>transiting system;  $i = 86.1^\circ \pm 0.1$  (Mazeh et al. 2000)

<sup>e</sup>closest of three known planets in the system

Table 2. Ephemerides, July 2002

Star	HJD at $\phi = 0$ days	$\delta(\text{HJD})^a$ days	Revised $P_{orb}$ days	$\delta(P_{orb})^a$ days
$\tau$ Boo	2452478.770	0.099	3.31245	0.00033
HD 179949	2452479.823	0.093	3.09285	0.00056
HD 209458	2452481.129	0.106	3.52443	0.00045
51 Peg	2452481.108	0.127	4.23067	0.00024
$\nu$ And	2452481.889	0.139	4.61794	0.00064

<sup>a</sup>uncertainties in the respective measurements

presumably acoustic waves which depend on  $T_{eff}$  and  $g$ . The integrated flux of the mean, normalized Ca II K core, including the photospheric contribution and the chromospheric emission, is listed in Table 1 and plotted against  $v\sin i$  in Figure 2. Even with the small number of program stars, there is a reasonable linear relationship between the two parameters as reported in Pasquini et al. (2000). HD 179949 lies significantly above the best-fit line. The Sun does as well, but this is known to be an effect of increased activity observed in the 2002 observing runs.<sup>2</sup>

The residuals of the normalized spectra (smoothed by 21 pixels) taken from the mean were used to generate the Mean Absolute Deviation ( $MAD = N^{-1}\Sigma|data_i - mean|$  for  $N$  spectra) plot shown in Figure 3 (top) for HD 179949. Superimposed on the plot is the corresponding K-core. The nightly residuals used to generate the MAD plot for HD 179949 are displayed just below. The activity seen in four of the five stars with planets, HD 179949,  $\tau$  Boo,  $v$  And and HD 209458, show significant deviations in the H & K reversals. The widths of the MAD plots (Figure 4) are the same as those of the reversals themselves as illustrated in Figure 3 for HD 179949. In the Sun’s case, images from the Michelson Doppler Imager (MDI) aboard the Solar Heliospheric Observatory (SOHO)<sup>3</sup> confirm that the sunspot group was receding which caused the apparent asymmetry of the solar MAD plot. The strong coherence between the H and K activity can be seen in Figure 5 where the integrated mean absolute deviation for H and K is plotted for each star. The strong aluminum line shows no comparable variations. For all the program stars, the mean absolute deviation of the Al I line at 3944Å is less than 0.0005 of the normalized mean. This indicates that the photospheres of the stars are stable to this level providing additional evidence that the variations seen in the Ca II H & K reversals are not caused by upper-level photospheric changes but rather are confined to the chromosphere.

## 5. HD 179949: A Convincing Case of Planetary-induced Modulation

HD 179949 shows the greatest nightly modulation of all the stars in all three observing runs. The integrated flux of the residuals shown in Figure 3 (bottom) are plotted against orbital phase in Figure 6. The emission clearly increases by  $\sim 4\%$  when the planet is in front of the star, at phases near the sub-planetary point ( $\phi \sim 0$ ) and is least when the

---

<sup>2</sup>We observed the naked-eye sunspot grouping of July 2002 in transit during our CFHT run with the Sunspotter<sup>®</sup> Solar Telescope supplied by the Visitor Information Center at the Onizuka Center for International Astronomy.

<sup>3</sup><http://sohowww.nascom.nasa.gov/> and <http://soi.stanford.edu/>

planet is behind the star ( $\phi \sim 0.5$ ). The amplitude and period of this activity has persisted during the year between observations (equal to 108 orbits or at least 37 stellar rotations). A periodogram of even these few data points (Stellingwerf 1978) produces the most significant peak with a period of 3 days.

### 5.1. Rotation of HD 179949

HD 179949 has no photometrically measured rotation period so, as derived from the  $v \sin i$ ,  $P_{rot} \leq 9$  days. The solid line in Figure 6 is a truncated, best-fit sine curve with  $P = P_{orb}$  corresponding to the change in projected area of a bright spot on the stellar surface before being occulted by the stellar limb. The peak of the model leads the sub-planetary point by 0.17 in phase. If this effect is real, it could provide a constraint on future models of the interaction. Since Ca II emission is optically thin outside the self-absorption core, limb brightening needs to be included in the model. According to solar observations discussed by Engvold (1966), limb brightening would increase emission by 3%, essentially not changing the geometric model.

The best-fit spot model requires the bright spot to be at a latitude of  $30^\circ$  and a stellar inclination angle  $i$  of  $87^\circ$ . Since there were no transits detected for this system, an upper limit for the orbital inclination is set at  $83^\circ$  (Tinney et al. 2001). The dashed model in Figure 6 has  $i = 83^\circ$  as it is generally assumed that the orbital and stellar inclination angles are comparable. These models are inconsistent with the possibility that the star may be tidally synchronized with the planet’s orbit ( $P_{rot} = P_{orb}$ ). However, from Figure 2, the Ca II K emission in HD 179949 is unusually strong compared to the other targets. This implies that either the inclination of the star is low,  $\sim 21^\circ$  ( $v \simeq 17.5 \text{ km s}^{-1}$  and  $P_{rot} \approx P_{orb} \approx 3 \text{ d.}$ ) or that  $P_{rot}$  is closer to 9 days and the Ca II emission is significantly enhanced in HD 179949 relative to the other stars.

If the star is indeed tidally synchronized with the planet, as is believed to be the case for  $\tau$  Boo, then the modulation in the emission observed with the 3.093-day period may be tracking a persistent stellar surface feature. However, tidal synchronization of HD 179949 is not a favoured scenario for two reasons. Firstly, the tidal synchronization timescale for the system  $\approx 700$  Gyr using a  $M_p \sin i = 0.84 M_J$ . (See Equation 1 of Drake et al. 1998). Even if  $i = 21^\circ$ , as would be the case for  $v = 17.5 \text{ km s}^{-1}$  and  $M_p = 2.34 M_J$ , then the synchronization timescale is still very long at 79 Gyr. Secondly, ROSAT X-ray data list HD 179949 as having at least double the X-ray flux (a measurement independent of  $i$ ) as compared to other single F8-9 dwarfs and  $\sim 10$  times that of the Sun’s. Hünsch et al. (1998) report the X-ray flux for HD 179949 to be  $L_X = 41.0 \times 10^{27} \text{ erg/s}$  while for 36 UMa, a nearly identical star,  $L_X$

$$= 18.4 \times 10^{27} \text{ erg/s} .$$

## 6. Summary

From the sample of stars observed, those with planets (with the exception of 51 Peg) show significant nightly variation in their Ca II H & K cores.  $\tau$  Ceti which has no close planet remained very steady over all three observing runs. The Sun's Ca II emission was stable within each run. However, a large naked-eye sunspot grouping appeared in the summer of 2002 and was detected as an enhancement in the H & K reversals accounting for its MAD signal (Figure 4). There is enhanced nightly activity in the stars with close-in giant planets whose variations may be cyclical and phase shifted. Further observations of these systems at varying orbital phases are required.

In the one clear case, HD 179949 exhibits repeated phase-dependent activity with enhanced emission near the sub-planetary point and less emission half an orbit later. This is consistent with a magnetic heating scenario and may be a first indirect glimpse at a magnetosphere of an extrasolar planet. Additional Ca II observations are crucial to confirm the continuity of the magnetic interaction as well as to establish better phase coverage. Due to the nearly exact 3-day orbit, it is impossible to get many distinct phases during one observing season from the ground. Space based observations will not only increase the phase coverage, but will also allow observations of other activity diagnostics such as transition region and coronal lines in the UV and FUV. Such mapping of planet-induced activity at varying stellar atmospheric depths will allow characterization and quantification of the physical interaction between the magnetically heated layers of the star and the planet's magnetosphere.

Research funding from the Canadian Natural Sciences and Engineering Research Council (G.A.H.W. & E.S.) and the National Research Council of Canada (D.A.B.) is gratefully acknowledged. We are also indebted to the CFHT staff for their care in setting up the CAFE fiber feed and the Gecko spectrograph.



## REFERENCES

- Baliunas S.L. et al., 1995, ApJ, 438, 269.
- Butler, P., Marcy G., Williams, E., Hauser, H., Shirts, P., 1997 ApJ, 474, L115.
- Charbonneau, D., Brown, T., Latham, D., Mayor, M., Mazeh, T., 1999, ApJ., 529, 45.
- Charbonneau, D., Brown, T.M., Noyes, R.W., Gilliland, R.L., 2002, ApJ, 568, 377.
- Cuntz, M., Saar, S.H., Musielak, Z.E., 2000, ApJ, 533, 151.
- Drake, S.A., Pravdo, S.H., Angelini, L.; Stern, R.A, 1998, AJ, 115, 2122.
- Engvold, O., 1966, ApNr, 10, 101.
- Fekel, F.C., 1997, PASP, 109, 514.
- François, P., Spite, M., Gillet, D., Gonzalez, J.-F., Spite, F., 1996, A&A, 310, 13.
- Gray, D.F., 1982, ApJ, 255, 200.
- Gray, D.F., 1986, PASP, 98, 319.
- Groot, P. J., Pitters, A. J. M., van Paradijs, J., 1996, A&AS, 118, 545.
- Hünsch, M., Schmitt, J.H.M.M., Voges, W., 1998, A&AS, 132, 155.
- Linsky, J.L., 1980, ARA&A, 18, 439.
- Marcy, G., Butler, P., Williams, E., Bildsten, L., Graham, J., 1996, ApJ, 481, 926.
- Mazeh, T., Naef, D., Torres, G., Latham, D.W., Mayor, M., Beuzit, J.-L., Brown, T.M., Buchhave, L., Burnet, M., Carney, B.W., Charbonneau, D., Drukier, G., Laird, J.B., Pepe, F., Perrier, C., Queloz, D., Santos, N.C., Sivan, J.-P., Udry, S., Zucker, S., 2000, ApJ, 532, L55.
- Musielak, Z.E., Rosner, R., Stein, R.F., Ulmschneider, P., 1994, ApJ, 423, 474.
- Pasquini, L., de Medeiros, J.R., Girardi, L., 2000, A&A, 361, 1011.
- Saar, S.H., Cuntz, M., 2001, MNRAS, 325, 55.
- Schneider, J., *Extrasolar Planets Catalog*, <http://www.obspm.fr/encycl/catalog.html>.
- Stellingwerf, R.F., 1978, ApJ, 224, 953.

Tinney, C., Butler, P., Marcy, G., Jones, H., Penny, A., Vogt, S., Apps, K., Henry, C., 2000, ApJ, 551, L507.

Ulmschneider, P., Musielak, Z.E., 1998, A&A, 338, 311.

Vidal-Madjar, A., Lecavelier des Étangs, A., Désert, J.-M., Ballester, G., Ferlet, R., Hébrard, G., Mayor, M., 2003, Nature, 422, 143.

Walker, G.A.H., Shkolnik, E., Bohlender, D.A., Yang, S., 2003, PASP, submitted.

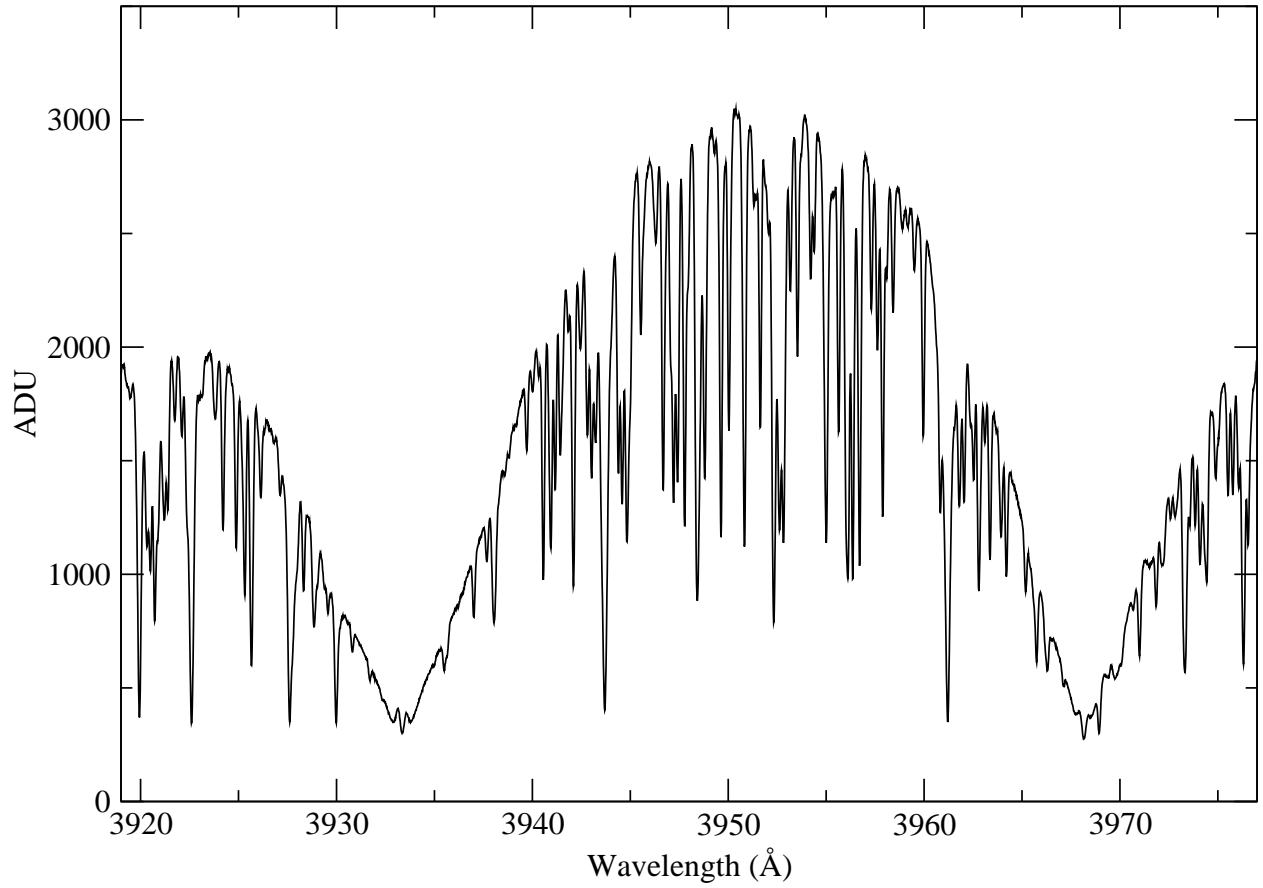


Fig. 1.— A single flat-fielded spectrum of HD 179949 taken over 40 minutes of integration time.

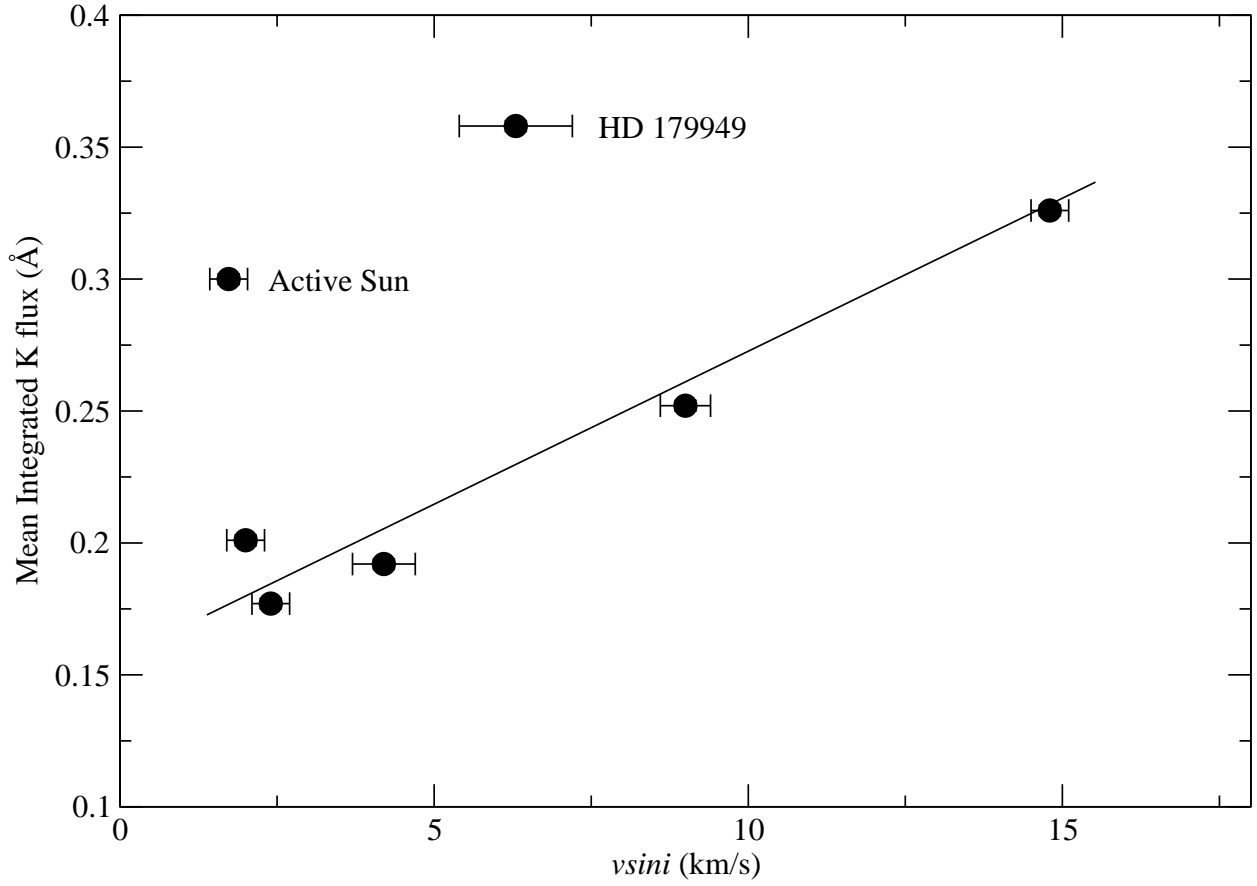


Fig. 2.— Published  $v \sin i$  values for the program stars (see Table 1) plotted against the integrated flux of the mean normalized Ca II K cores.

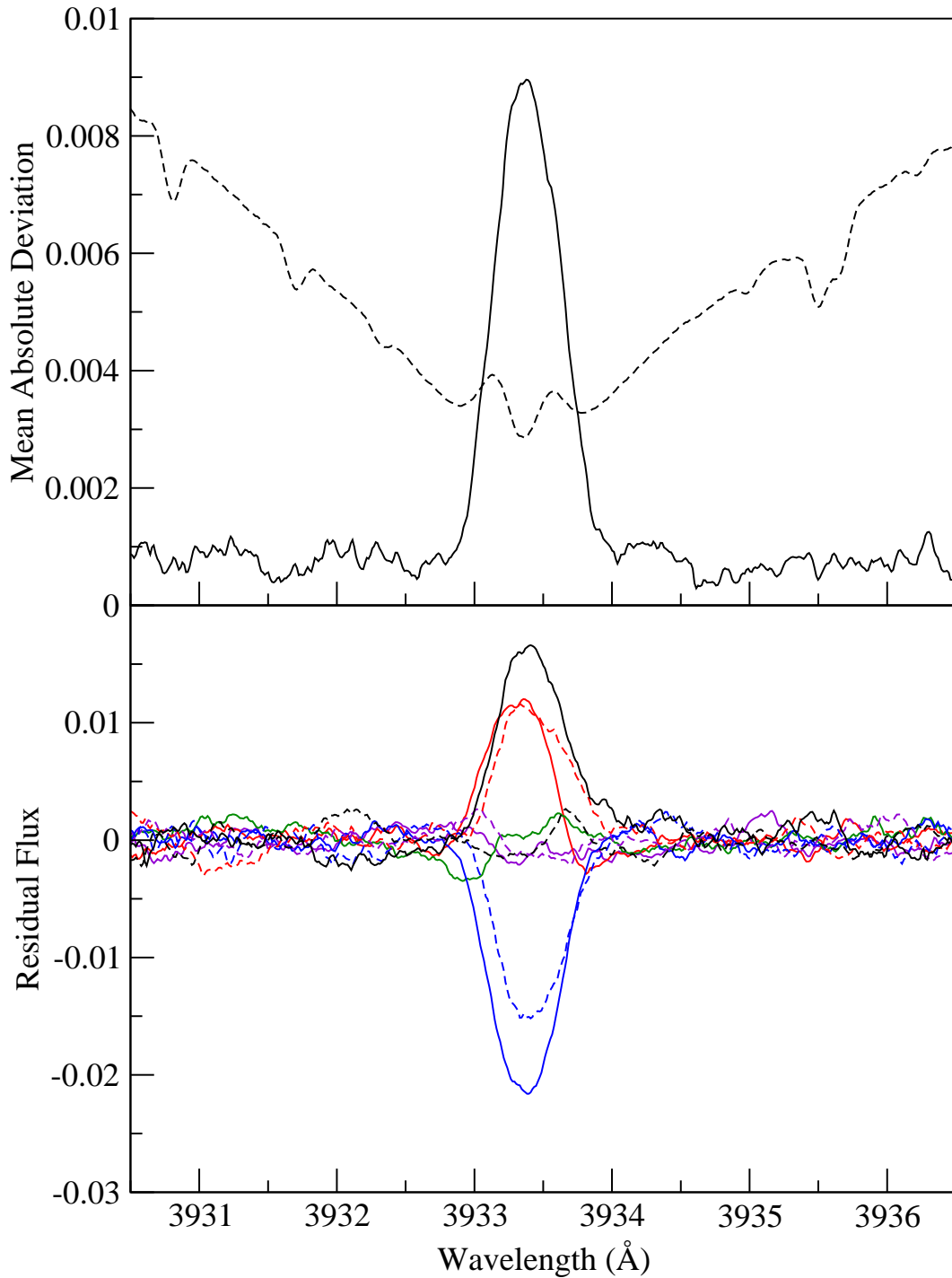


Fig. 3.— Top: The mean absolute deviation (MAD) of the Ca II K core (solid line) of HD 179949. The units are intensity as a fraction of the continuum. Overlaid (dashed line) is the overall mean spectrum indicating that the activity in HD 179949 is confined to the K emission. Bottom: Residuals (smoothed by 21 pixels) from the normalized mean spectrum of the Ca II K core of HD 179949. The residuals for the H line follow these closely.

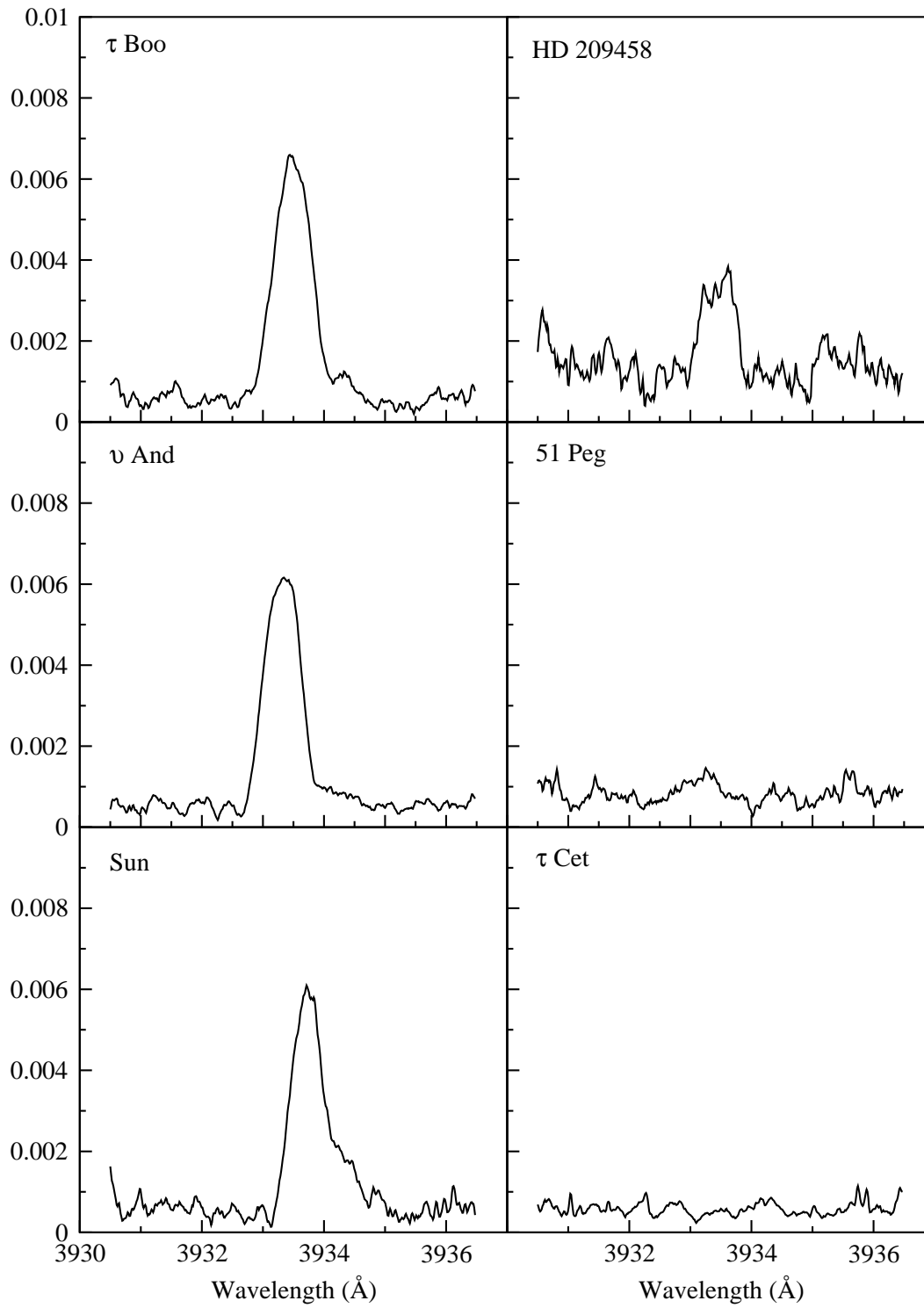


Fig. 4.— MAD plots for the other six program stars. Units are intensity as a fraction of the continuum.

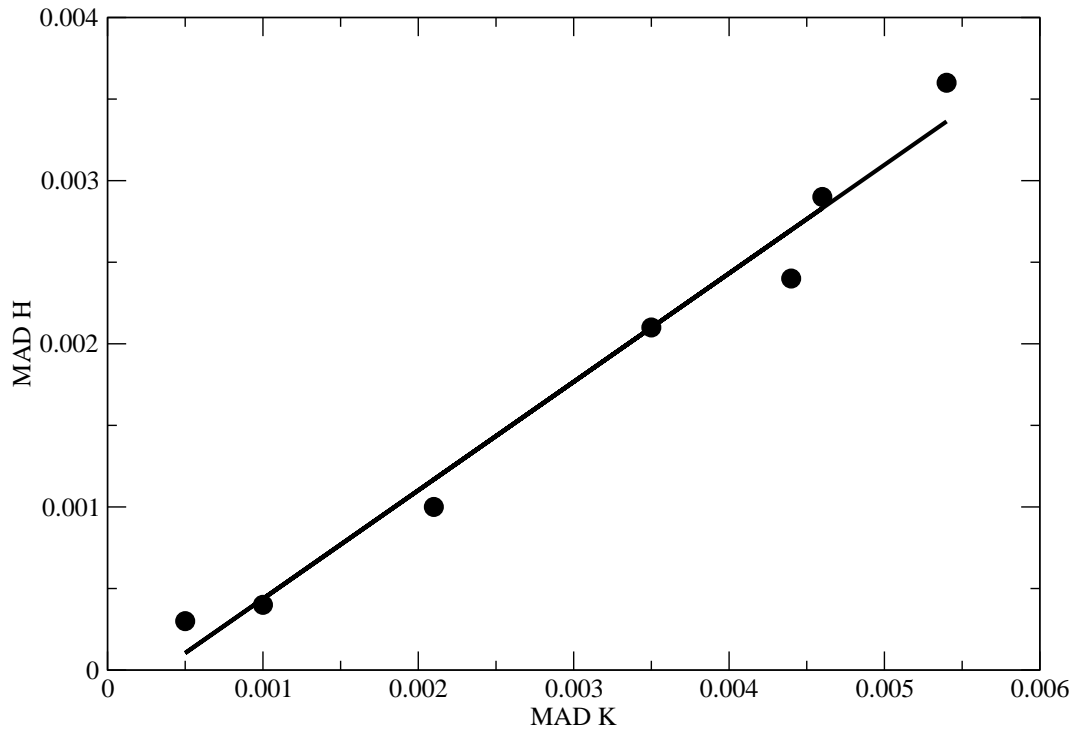


Fig. 5.— Integrated “intensity” of the MAD H and K plots for all the program stars. The slope of the best-fit line is 0.665.

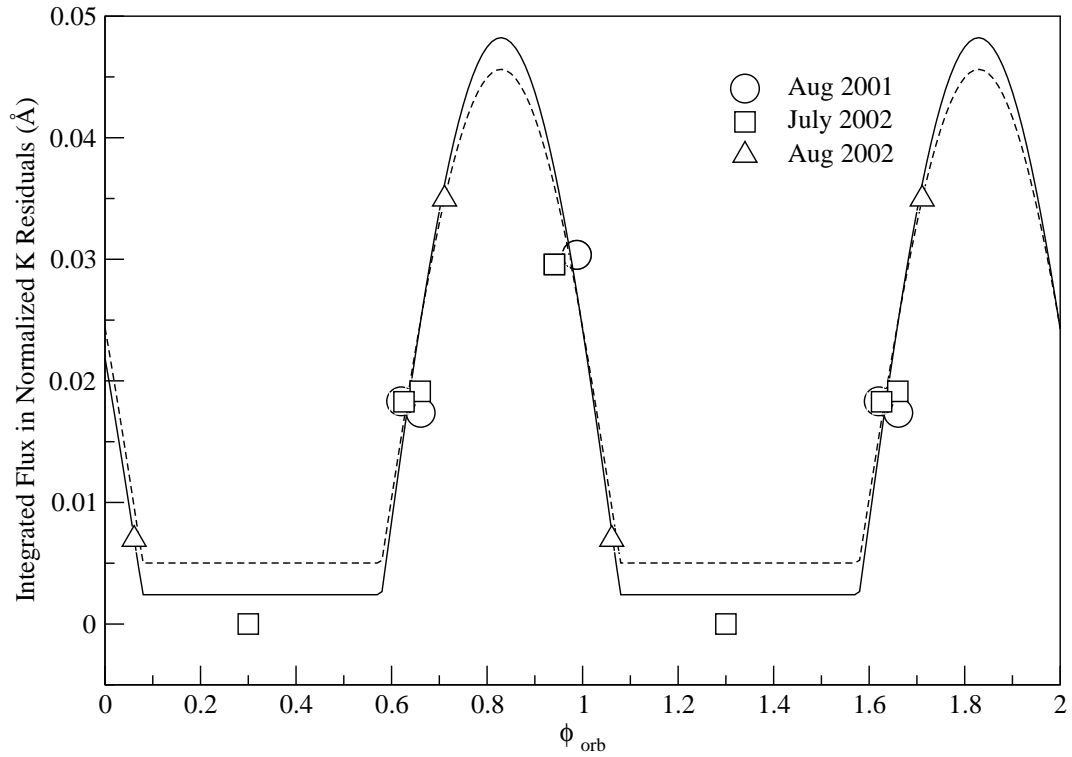


Fig. 6.— Integrated flux of the nine K-line residuals taken from a normalized mean spectrum. The minimum flux was set to zero and all others scaled accordingly. The size of the points is the size of the error bars. The solid line is the best-fit bright-spot model discussed in the text with the spot at a latitude of  $30^\circ$  and stellar inclination angle  $i = 87^\circ$ . The dashed line is a model with  $i = 83^\circ$